

pubs.acs.org/macroletters Letter

Porous Melt Blown Poly(butylene terephthalate) Fibers with High Ductility and High-Temperature Structural Stability

Joshua W. Goetze, Cesar Benitez, Frank S. Bates,* and Christopher J. Ellison*



Cite This: ACS Macro Lett. 2024, 13, 558-564



ACCESS

Metrics & More

Article Recommendations

Supporting Information

ABSTRACT: In this study, porous poly(butylene terephthalate) (PBT) fibers were produced by melt blowing cocontinuous blends of PBT and polystyrene (PS) and selectively extracting the interconnected PS domains. Small amounts of hydroxyl terminated PS additives that can undergo transesterification with the ester units in PBT were added to stabilize the cocontinuous structure during melt processing. The resulting fibers are highly ductile and display fine porous structural features, which persist at temperatures over 150 °C. Single fiber tensile testing and electron microscopy are presented to demonstrate the role of rapid

Porous PBT Melt Blown Fibers

10 µm

150 °C

Stretch

5 µm

Thermal
Pore Stability

Single Fiber
Ductility

quenching and drawing of the melt blowing process in defining the fiber properties. The templated highly aligned pore structure, which is not easily produced in solvent-based fiber spinning methods, leads to remarkable mechanical properties of the porous fibers and overcomes the notoriously poor tensile properties common to other cellular materials like foams.

onwovens are a class of fibrous mats that consist of randomly oriented patrice. mats are used extensively in fields ranging from everyday consumer products to high performance separations, biomedical devices,^{3,4} and battery electrodes.⁵ Melt blowing is a widely used method for producing nonwovens that involves extrusion of molten polymer through small orifices to form filaments that are rapidly stretched by impinging jets of heated air into micron or nanoscale fibers.⁶⁻⁸ The process is readily scalable and enables high-throughput production while avoiding the large amounts of flammable solvent necessary in other fiber formation methods, such as electrospinning or blow spinning. Generally, melt blowing feed materials consist of a single polymer such as polypropylene, polystyrene (PS),9 poly(butylene terephthalate) (PBT), 8,10 or poly(lactic acid), 11 resulting in single component fibers with simple circular cross sections and smooth fiber surfaces.

Incorporating surface roughness, chemical surface modification, or internal porosity into melt blown fibers can enable further refinement of properties for filtration and coalescence media or bring the high throughput and efficiency of melt blowing to higher value applications, including drug delivery and water remediation. Early work tuning melt blown fiber surface properties involved post-treatment steps such as hydrolysis of polyester nonwovens to produce nanoscale surface roughness and modify the surface chemistry. Fibers can be further modified to enable anisotropic wetting allow loading of active materials Incorporating oriented surface structures or internal porosity. These types of structures are almost exclusively produced using electrospinning with nonsolvent induced phase separation forming

the pores. ^{15–17} However, electrospinning often requires dissolution of the feed polymer in a solvent (often <20 wt % polymer), ¹⁸ limiting the throughput and types of polymers compatible with the process. ³ Developing and evaluating alternative methods to achieve such structures is highly desirable.

Recently, Banerji et al. demonstrated porous fiber production by melt blowing cocontinuous blends composed of a sacrificial, solvent-extractable PS phase and a semicrystal-line polyethylene phase. In contrast to discontinuously dispersed blends, where one component encapsulates droplets of the other, cocontinuous blends have two interpenetrating domains. Upon melt blowing, the cocontinuous blends retained interconnectivity, allowing near full extraction of the PS with a selective solvent. Using this method, the authors were able to produce porous polyethylene melt blown fibers with highly oriented and interconnected nanoscale pores. In

In evaluating the utility and limitations of this method, the thermal and mechanical stability of the porous fiber product must be considered.^{6,7} In high-temperature environments, where nonstructured fibers could show small changes in fiber diameter due to microstructural rearrangement, the fine features on and within porous fibers may change or collapse

Received: February 12, 2024 Revised: April 10, 2024 Accepted: April 10, 2024



entirely.²¹ Additionally, foams and other types of porous solids generally have notoriously poor tensile properties, even when composed of highly ductile materials. ^{21–24} For nonwovens, characterizing the role of fiber structure on mechanical properties is best determined through single fiber tensile tests, which provide the most direct information without convoluting nonwoven mat characteristics such as fiber-to-fiber bonding or mat density. Previous single fiber testing, however, has been almost entirely focused on nonporous fibers. 11,25-A notable exception is work by Li et al., where the properties of porous electrospun polylactide fibers produced from different electrospinning setups were characterized but the mechanistic role of the porous structure was not elucidated. The comparatively large differences in processing characteristics between rapid solvent evaporation in electrospinning and rapid thermal quenching in melt blowing^{6,7} further motivates mechanical tests of porous melt blown fibers.

In this report, we demonstrate the production of porous melt blown fibers composed of PBT, a resin commonly used for melt blowing due to its resistance to a wide range of solvents and its high melting temperature. Importantly, the solvent resistance makes producing PBT fibers by solution-based methods challenging and expensive. ^{3,18} In the melt state, PBT is readily processable with ester functionalities that enable simple reactive compatibilization with other polymers. ³⁰ We demonstrate the thermal stability of templated pore structures produced from PS/PBT cocontinuous blends and, for the first time, perform single fiber tensile tests on porous melt blown fibers, characterizing their ductility and revealing remarkable retention of mechanical properties relative to nonporous fibers.

Here, porous PBT fibers were produced in a manner similar to that reported by Banerji et al. through melt blowing cocontinuous blends of PBT (Celanex 2008) and a sacrificial PS (Sigma-Aldrich 43011-0, $M_n \cong 100$ kDa, D = 2.24). PBT and PS pellets were dried under vacuum for 4 h at 125 °C and 12 h at 150 °C, respectively, before processing. Blends were produced in a conical twin screw microcompounder (Xplore 15 cc) at 265 °C with a 60:40 PS:PBT solid volume ratio (assuming PS and PBT densities of 1.04 and 1.3 g/cm³, respectively^{31,32}) and quenched in a cold-water bath. The unequal volume fractions are necessary to achieve cocontinuity due to the PS having a significantly higher melt viscosity (see Supporting Information). Blends were cut into pellets, dried for 4 h at 125 °C under vacuum, and melt blown with polymer and air temperatures of 265 °C using a 0.1 mm orifice on a custom lab scale melt blowing system, which has been described previously. Polymer and air flow rates were 0.9 g/ min/hole and 4.5 standard cubic feet per minute, respectively, producing high aspect ratio fibers with minimal defects. After melt blowing, the PS domains were extracted by soaking the mats in 40 °C cyclohexane overnight and drying under vacuum at 50 °C overnight to yield porous PBT fibers. The cocontinuous blend templating method is depicted in Figure 1, with scanning electron microscopy (SEM) images displaying the initial blend morphology and the final porous fiber surface and cross-sectional features after extraction of the PS phase.

One challenge of working with cocontinuous blends is the propensity for the morphology to rapidly coarsen when held in the melt state.³³ Such coarsening can be largely arrested through the use of compatibilizers like block copolymers.^{19,33} Here monohydroxy-terminated PS (PS–OH) is added, which due to the high processing temperature (265 °C) can react with ester groups on the PBT chain to form *in situ*

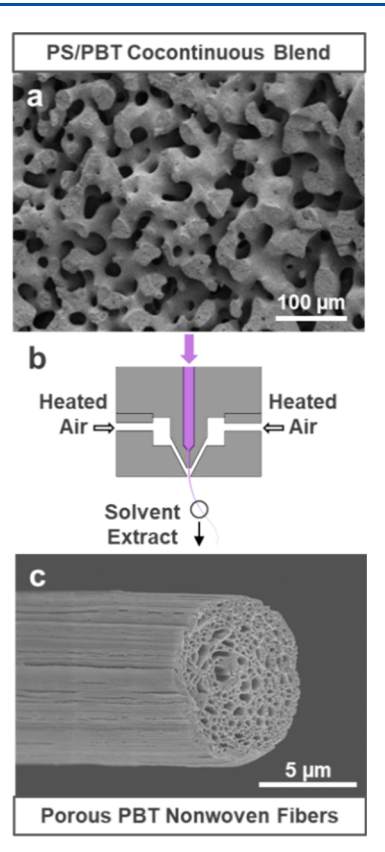


Figure 1. (a) SEM image of cocontinuous PS/PBT blend prior to melt blowing and after PS domain solvent extraction, (b) schematic of the melt blowing process, and (c) SEM image of a fractured porous PBT fiber product.

copolymers³⁰ without added catalyst. The PS–OH additives used here have >85% hydroxy end group functionality as characterized by nuclear magnetic resonance spectroscopy (see Supporting Information). Various loadings of either 50 or 10 kDa PS–OH were blended with PBT for 5 min before adding unfunctionalized PS to obtain a 60:40 PS/PS–OH:PBT volume fraction and blending for another 6 min. The coarsening rate was then evaluated by melt pressing samples of the blends and holding them at the melt blowing temperature (265 °C) for various times before quenching and imaging. Domain size was quantified by measuring the domain area, A, and perimeter, P, in multiple SEM images using ImageJ analysis software and defining the characteristic length, D = 4A/P.

The rapid growth in domain size during the annealing of the uncompatibilized 60:40 PS:PBT blends is shown in Figure 2a. Blends with 5 wt % (relative to the total blend mass) of either the 50 or 10 kDa PS-OH show dramatically reduced domain coarsening and still exhibit the cocontinuous morphology. At the same mass loadings, the 10 kDa PS-OH coarsens less than the 50 kDa PS-OH, most noticeably at 1 wt % (Figure 2b). Notably, the 10 kDa additive corresponds to roughly 5× the number of chains, so the increase in efficiency may simply be associated with higher interfacial coverage and a subsequent decrease in interfacial tension. For melt blowing, 60:40 PS/PS-OH:PBT blends with 5 wt % 10 kDa PS-OH were used (highlighted in purple in Figure 2). These blends strike a balance between the enhanced stability of the cocontinuous structure and the expected higher cost of the reactive additive.

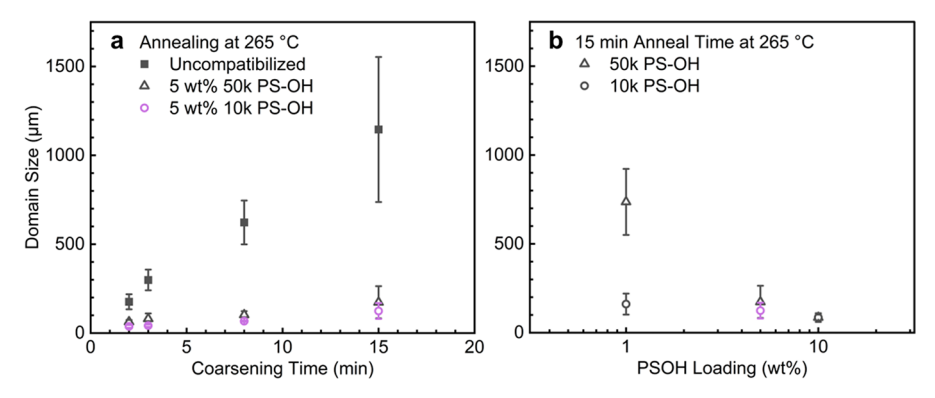


Figure 2. Domain size coarsening of cocontinuous 60:40 vol PS:PBT blends during annealing at 265 °C. (a) Growth in domain size with time for uncompatibilized and 5 wt % PS-OH blends. (b) Impact of PS-OH loading on domain size after 15 min of coarsening. Purple symbols show data for the blend composition used for melt blowing. Error bars are the 95% confidence interval.

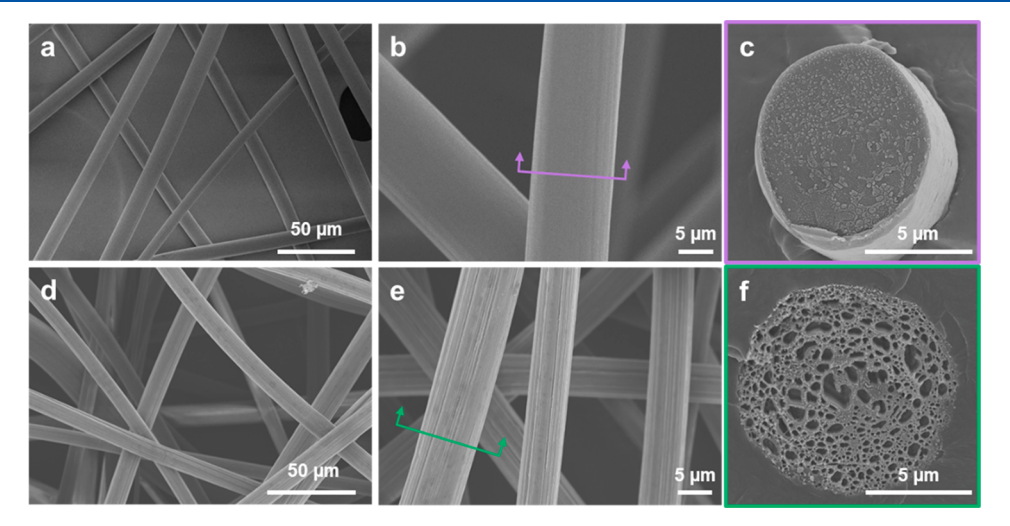


Figure 3. SEM images of fibers melt blown from 60:40 PS:PBT blends with 5 wt % 10 kDa PS-OH using different magnifications and viewpoints (a-c) before and (d-f) after extraction of PS domains. Arrowed brackets indicate viewpoint direction corresponding to the color-coded cross section image to the right.

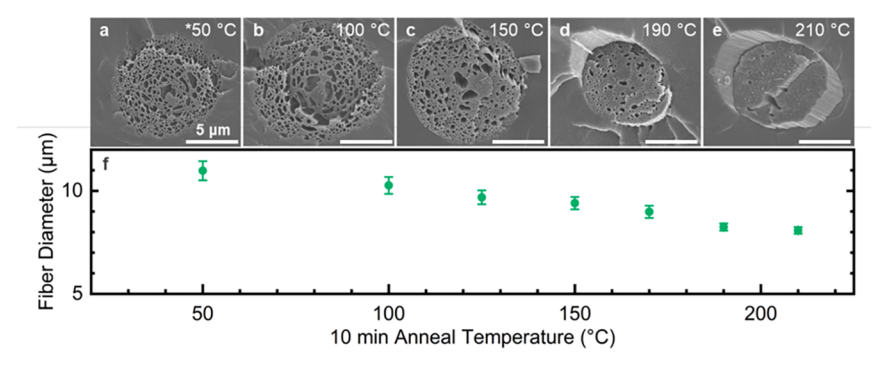


Figure 4. (a-e) Cross-sectional SEM images of porous fibers annealed at various temperatures and (f) evolution of fiber diameter against annealing temperature. Error bars correspond to a 95% confidence interval. *The 50 °C sample represents the fibers after drying overnight prior to annealing in the N_2 environmental chamber.

After melt blowing, the as-spun cocontinuous blend fibers had an average diameter of $10.9 \pm 0.2~\mu m$ as characterized by SEM, based on the measurement of at least 130 fibers. Figure 3a-c display representative SEM images of the blend fiber mat structure, fiber surface, and fiber cross section obtained by fracturing fibers embedded in epoxy while immersed in liquid nitrogen. The blend fibers exhibit slightly grooved surfaces, which are not observed in fibers produced at the same conditions using pure PBT or PS. These structures have also

been observed in melt spun fibers of immiscible blends,³⁴ so we suggest they may result from differences in coefficients of thermal expansion between the PS and PBT phases or a preference for the PS domain to locate at the surface. In the cross-sectional images, the PS and PBT domains can be distinguished by the different fracture textures.

After extraction of PS, the mat mass decreased by 47 \pm 2%, which corresponds to 96 \pm 3% of the uncompatibilized PS based on the bulk composition. The near quantitative

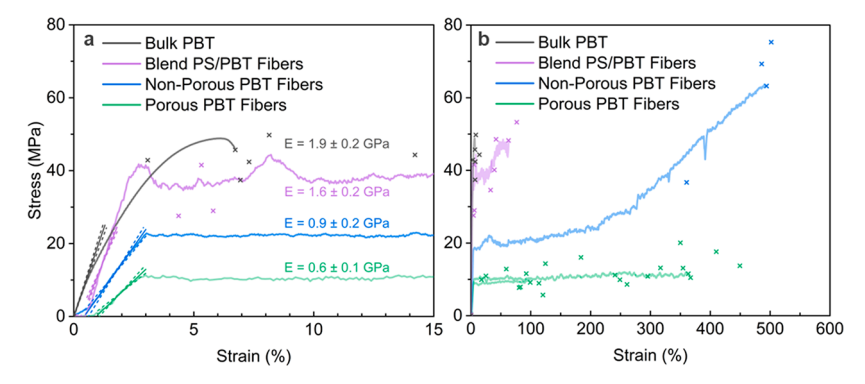


Figure 5. Representative stress—strain data of melt pressed PBT tensile bars and single melt blown nonporous, blend, and porous fibers at (a) small strain and (b) large strain. Strain-at-break for all samples tested are marked by (\times) symbols matching the sample color. Lines show the fit of initial deformation for determination of the elastic modulus with dotted lines showing a 95% confidence interval of the mean.

extraction of PS indicates retention of the PS domain connectivity in the melt blown fibers. SEM images of the porous fiber mat structure, fiber surface, and cross-section are displayed in Figure 3d–f.

The porous fibers show highly oriented grooved surface structures with a characteristic width of ~100 nm. Crosssectional imaging displays larger pores on the order of 1 μ m near the center of the fiber, which decrease in diameter radially. This decreasing pore size may be due to the higher shear rate at the fiber surface during stretching after exiting the die, or more likely, the higher shear rate at the wall of the melt blowing orifice in the die,⁷ which may be as high 10⁵ s⁻¹ for this system if there is minimal wall or interfacial slip^{35,36} (see Supporting Information). These high shear rates and the appearance of a high melting shoulder in the first heating differential scanning calorimetry (DSC, see Supporting Information) suggest some level of stress-induced crystallization may be occurring,³⁷ however, we do not think this plays a large role in defining the pore morphology. Significantly, these fibers were embedded and fractured after the PS was extracted from the bulk fiber mat. Due to the extremely high aspect ratio of the fibers, PS extraction must occur through radial connections between pores. Several such connections can be seen in the fiber shown in Figure 1c.

In applications involving fuel and oil filtration, nonwoven media can be exposed to temperatures as high as 150 °C. To evaluate the stability of the nanoscale structural features, porous fibers were annealed as a mat at temperatures ranging from 100 to 210 $^{\circ}\text{C}$ for 10 min in a TA Instruments ARES-G2 rheometer environmental chamber under nitrogen. SEM images of cross sections of the annealed fibers (Figure 4a-e) indicate a decrease in porosity as the fibers are heated above 150 °C. Fiber morphology was tracked quantitatively by measuring the average fiber diameter of samples annealed over the range of temperatures. Figure 4f displays the decrease in fiber diameter from 11.0 \pm 0.4 to 8.1 \pm 0.2 μ m between the unannealed and 210 °C annealed samples. This change in diameter corresponds to a decrease in the average fiber crosssectional area of just over 45%, which provides a rough lower bound of the porosity of the fibers.

Noting that the melting temperature of PBT crystals is approximately 225 °C, the pore collapse is attributed to some form of microstructural rearrangement as the fibers are heated above the PBT glass transition temperature, $T_{\rm g,PBT}=60$ °C. A first heat DSC trace (see Supporting Information) displays no consolidated exotherm, indicating no cold crystallization

occurs from a quenched and arrested amorphous state. Instead, we propose small, poorly developed crystalline domains gradually restructure into larger $\alpha\text{-crystals}$. This mechanism is supported by X-ray scattering profiles of the annealed fiber samples (see Supporting Information), which show broad features in the unannealed samples and well-developed peaks in the 190 and 210 $^{\circ}\text{C}$ annealed samples, all matching the $\alpha\text{-crystal}$ peak positions. The crystalline order that develops upon thermal annealing has also been observed in electrospun PBT fibers, 18 suggesting there is some similarity in the fiber microstructure despite the different fiber spinning methods.

Minimal development of crystals in the unannealed fibers is a product of rapid quenching during melt blowing from 265 °C to near or below $T_{\rm g,PBT}$ (60 °C). In addition to impacting the thermal stability, high amorphous content or sufficiently small crystalline domains will also lead to dramatic changes in the mechanical properties of the polymer.³⁹⁻⁴¹ To understand how the thermal history and macroscopic pores impact fiber mechanical properties, single fiber tensile tests were conducted using an RSA-G2 instrument (TA Instruments). Three types of fibers with similar average diameters (d_{avg}) were compared to melt pressed PBT films (cut into tensile bars), which provide a reference for the bulk polymer properties (Figure 5). The fiber samples include porous fibers ($d_{avg} = 12 \pm 4 \mu m$), cocontinuous PS/PBT blend fibers ($d_{avg} = 10 \pm 4 \mu m$), both made with 5 wt % 10 kDa PS-OH, and nonporous PBT fibers $(d_{\text{avg}} = 14 \pm 3 \,\mu\text{m})$. The last of which was melt blown using the pure PBT resin with a lower air temperature of 240 $^{\circ}\text{C}$ to achieve comparable fiber diameters. Figure 5a,b displays representative stress-strain data for each of the sample types, with Figure 5a highlighting the low strain portion of each test. Engineering stress was calculated using the equation $\sigma = F/A_{\rm o}$, where F is the applied force and $A_{\rm o}$ is the initial sample cross sectional area. For the fiber samples, A_0 was determined from diameters measured by optical microscopy and assuming a circular cross section. Area was not corrected for the pore fraction in the porous fibers.

Comparing the bulk PBT and nonporous PBT fibers provides insight into the role of processing history imparted by melt blowing. Bulk PBT shows characteristic brittle behavior, with all samples failing below 15% strain and a modulus of 1.9 \pm 0.2 GPa. The modulus of the nonporous pure PBT fibers was half that of the bulk material at 0.9 \pm 0.2 GPa. However, the fibers displayed remarkable ductility, deforming up to 500% strain in some samples. Similar to the

porous fibers, the nonporous PBT fibers show minimal crystal development (see X-ray scattering in the Supporting Information), which likely contributes to this difference in mechanical properties. The fiber stress—strain tests show yielding then necking at $\sigma\cong 22$ MPa followed by extensive strain hardening, behavior similar to deformation of melt spun PBT fibers produced at low take-up velocities. However, the melt blown fibers show half the plateau stress of the melt spun fibers.

The PS/PBT fibers exhibited a higher modulus of 1.6 \pm 0.2 GPa, reflecting the presence of rigid glassy PS domains. These fibers failed at much lower elongation than the nonporous PBT, often only reaching 50–100% strain, with some failing at as low as 5% strain. The low ductility is similar to behavior of bulk immiscible blends, particularly in cases where one component changes density substantially more than the other component upon cooling (e.g., blends containing a semicrystalline and amorphous polymer). 30,43 For these blends, the region of cocontinuity has been noted to display particularly brittle properties.⁴³ Toughness of such blends can be improved by compatibilization. 30 However, two factors act against the efficacy of PS-OH in the PS/PBT blend fibers examined here: (1) The PS-OH polymer ($M_n = 10 \text{ kDa}$) is below the entanglement molecular weight, $M_{e,PS}$, 13 kDa; (2) There is likely low interfacial coverage due to the large and rapid increase in interfacial area between the domains associated with fiber formation.

Once the PS domains are extracted to produce porous fibers, the modulus decreases substantially to 0.6 ± 0.1 GPa, but remarkably, the fibers again show high ductility, deforming to several hundred percent strain before breaking. However, the porous fibers display much greater variability in strain-at-break and a higher density of necking regions (Figure 6a,b), which we attribute to heterogeneities in the pore structure or unextracted PS inclusions.

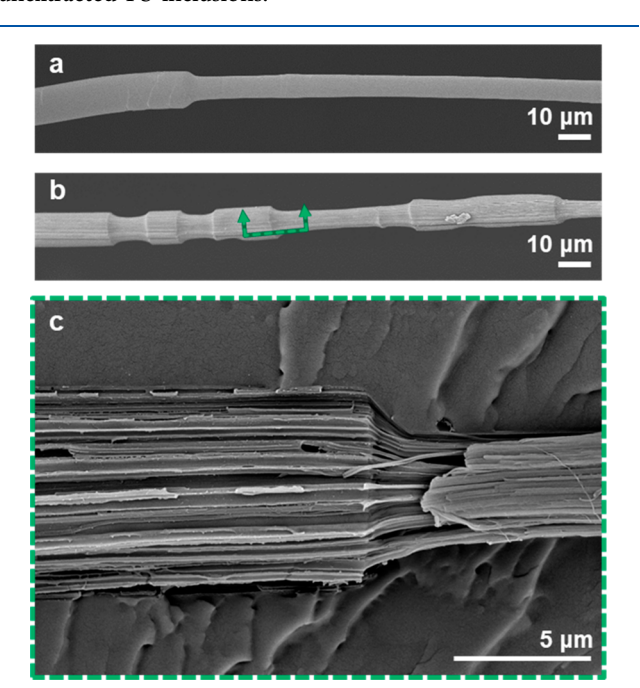


Figure 6. Representative SEM images of necking behavior of (a) nonporous and (b) porous fibers deformed to 50% strain. (c) Cross-section of neck on a porous PBT fiber, embedded in epoxy, in a region like that indicated by arrows in (b).

Nonetheless, the observed ductility is in stark contrast to other cellular solids, even those composed of highly ductile polymers, which are often brittle in tension. 23,44 We propose that this ductility is related to the high alignment and aspect ratio of the pore structure. The morphology is similar to lotusroot-type porous structures produced in metals and ceramics, which have aligned cylindrical pore structures and show dramatic anisotropy in their tensile properties. 45,46 Tensile loading perpendicular to the pore axis results in brittle properties akin to other cellular materials, while loading parallel to the pore axis shows ductility similar to that of the bulk material. Notably, the tensile modulus of these materials scales with the solid cross-sectional area. 47,48 This scaling is also observed between the moduli of nonporous and porous fibers (solid volume fraction of ~0.55) along with a similar scaling of the plateau stress. Deformation of the aligned pores is shown in Figure 6c and illustrates the sharp change in pore shape as material is pulled into the neck region, enabling ductility. In contrast, PS/PBT blend fibers before PS removal are characteristically brittle because fracture of the continuous PS phase likely results in subsequent deformation being localized to near the fracture site, requiring the load to be solely supported by surrounding PBT. Drawing of more PBT into the deformation region in the manner shown in Figure 6c for porous fibers is accordingly impeded by the remaining PS structure in PS/PBT blend fibers, 49 leading to rapid failure.

In conclusion, cocontinuous blends of PBT and PS, stabilized by PS-OH can be melt blown into 5-10 μ m fibers. Selective extraction of the PS produces highly oriented submicron pore structure, which is stable to over 150 °C. These porous PBT fibers exhibit densely segmented necking under tension and surprising ductility in contrast to the brittle nature of the bulk material and other cellular solids. We attribute these remarkable properties to the rapid quenching and highly anisotropic pore structure, the latter of which is not easily produced by solvent-based fiber forming methods but is inherent to the melt blowing process. We hypothesize that the cocontinuous blend system and process demonstrated here could be readily adapted to other high melting polyesters or a water extractable sacrificial phase like poly(ethylene oxide) to further tune the fiber structure, stability, and surface functionalization. This pore templating method provides a useful tool for tuning melt blown fiber morphology, which could expand the application of this important class of plastics.

ASSOCIATED CONTENT

Supporting Information

The Supporting Information is available free of charge at https://pubs.acs.org/doi/10.1021/acsmacrolett.4c00093.

Materials, pure component characterization, sample preparation details, and additional characterizations, including DSC and WAXS (PDF)

AUTHOR INFORMATION

Corresponding Authors

Christopher J. Ellison – Department of Chemical Engineering and Materials Science, University of Minnesota, Minneapolis, Minnesota 55455, United States; orcid.org/0000-0002-0393-2941; Email: cellison@umn.edu

Frank S. Bates – Department of Chemical Engineering and Materials Science, University of Minnesota, Minneapolis,

Minnesota 55455, United States; oorcid.org/0000-0003-3977-1278; Email: bates001@umn.edu

Authors

Joshua W. Goetze – Department of Chemical Engineering and Materials Science, University of Minnesota, Minneapolis, Minnesota 55455, United States

Cesar Benitez – Department of Mechanical Engineering, University of Texas Rio Grande Valley, Edinburg, Texas 78539, United States

Complete contact information is available at: https://pubs.acs.org/10.1021/acsmacrolett.4c00093

Author Contributions

CRediT: Cesar Benitez investigation; Joshua W. Goetze investigation, methodology, writing — original draft; Frank S. Bates conceptualization, funding acquisition, writing — review & editing; Christopher J. Ellison conceptualization, funding acquisition, writing — review & editing.

Funding

This work was funded and supported by Cummins Filtration (now Atmus Filtration), the Partnership for Research and Education in Materials (PREM) Program of the National Science Foundation under Award Number DMR-2122178, and the University of Minnesota MRSEC under Award Number DMR-2011401.

Notes

The authors declare no competing financial interest.

ACKNOWLEDGMENTS

The authors thank Dr. Aaron Lindsay for synthesizing the 50 kDa hydroxy-terminated polystyrene used in this work. Parts of this work were carried out in the Characterization Facility, University of Minnesota, which receives partial support from the NSF through the MRSEC (Award Number DMR-2011401) and the NNCI (Award Number ECCS-2025124) programs. NMR instruments were purchased and maintained with support from the Office of Vice President Research, College of Science and Engineering, and the Department of Chemistry at the University of Minnesota.

REFERENCES

- (1) Arouni, H.; Farooq, U.; Goswami, P.; Kapur, N.; Russell, S. J. Coalescence Efficiency of Surface Modified PBT Meltblown Nonwovens in the Separation of Water from Diesel Fuel Containing Surfactants. *Results in Engineering* **2019**, *4*, No. 100048.
- (2) Wang, K.; Haberkamp, W. C. Nonwoven Web with Bimodal Fiber Distribution. U.S. Patent No. US2020/0354869A1, November 12, 2020.
- (3) Tuin, S. A.; Pourdeyhimi, B.; Loboa, E. G. Creating Tissues from Textiles: Scalable Nonwoven Manufacturing Techniques for Fabrication of Tissue Engineering Scaffolds. *Biomedical Materials (Bristol)* **2016**, *11* (1), 015017.
- (4) Park, J. Y.; Lee, I. H. Controlled Release of Ketoprofen from Electrospun Porous Polylactic Acid (PLA) Nanofibers. *Journal of Polymer Research* **2011**, *18* (6), 1287–1291.
- (5) Liu, C.; Li, Q.; Kang, W.; Lei, W.; Wang, X.; Lu, C.; Naebe, M. Structural Design and Mechanism Analysis of Hierarchical Porous Carbon Fibers for Advanced Energy and Environmental Applications. *J. Mater. Chem. A Mater.* **2021**, *10* (1), 10–49.
- (6) Shambaugh, R. L. A Macroscopic View of the Melt-Blowing Process for Producing. *Ind. Eng. Chem. Res.* **1988**, 27, 2363.

- (7) Drabek, J.; Zatloukal, M. Meltblown Technology for Production of Polymeric Microfibers/Nanofibers: A Review. *Phys. Fluids* **2019**, *31* (9), No. 091301.
- (8) Ellison, C. J.; Phatak, A.; Giles, D. W.; Macosko, C. W.; Bates, F. S. Melt Blown Nanofibers: Fiber Diameter Distributions and Onset of Fiber Breakup. *Polymer* **2007**, *48* (11), 3306–3316.
- (9) Tan, D. H.; Zhou, C.; Ellison, C. J.; Kumar, S.; Macosko, C. W.; Bates, F. S. Meltblown Fibers: Influence of Viscosity and Elasticity on Diameter Distribution. *J. Nonnewton Fluid Mech* **2010**, *165* (15–16), 892–900.
- (10) Wang, Z.; Macosko, C. W.; Bates, F. S. Tuning Surface Properties of Poly(Butylene Terephthalate) Melt Blown Fibers by Alkaline Hydrolysis and Fluorination. ACS Appl. Mater. Interfaces 2014, 6 (14), 11640–11648.
- (11) Liu, G.; Guan, J.; Wang, X.; Yu, J.; Ding, B. Polylactic Acid (PLA) Melt-Blown Nonwovens with Superior Mechanical Properties. *ACS Sustain Chem. Eng.* **2023**, *11*, 4279–4288.
- (12) Wang, Z.; Macosko, C. W.; Bates, F. S. Tuning Surface Properties of Poly(Butylene Terephthalate) Melt Blown Fibers by Alkaline Hydrolysis and Fluorination. *ACS Appl. Mater. Interfaces* **2014**, *6* (14), 11640–11648.
- (13) Liang, M.; Chen, X.; Xu, Y.; Zhu, L.; Jin, X.; Huang, C. Double-Grooved Nanofibre Surfaces with Enhanced Anisotropic Hydrophobicity. *Nanoscale* **2017**, *9* (42), 16214–16222.
- (14) Farzan, M.; Roth, R.; Schoelkopf, J.; Huwyler, J.; Puchkov, M. The Processes behind Drug Loading and Release in Porous Drug Delivery Systems. *Eur. J. Pharm. Biopharm.* **2023**, *189*, 133–151.
- (15) Fashandi, H.; Karimi, M. Characterization of Porosity of Polystyrene Fibers Electrospun at Humid Atmosphere. *Thermochim. Acta* **2012**, 547, 38–46.
- (16) Li, Y.; Lim, C. T.; Kotaki, M. Study on Structural and Mechanical Properties of Porous PLA Nanofibers Electrospun by Channel-Based Electrospinning System. *Polymer* **2015**, *56*, 572–580.
- (17) Medeiros, E. S.; Mattoso, L. H. C.; Offeman, R. D.; Wood, D. F.; Orts, W. J. Effect of Relative Humidity on the Morphology of Electrospun Polymer Fibers. *Can. J. Chem.* **2008**, *86* (6), 590–599.
- (18) Wang, C.; Fang, C. Y.; Wang, C. Y. Electrospun Poly(Butylene Terephthalate) Fibers: Entanglement Density Effect on Fiber Diameter and Fiber Nucleating Ability towards Isotactic Polypropylene. *Polymer* **2015**, *72*, 21–29.
- (19) Banerji, A.; Jin, K.; Mahanthappa, M. K.; Bates, F. S.; Ellison, C. J. Porous Fibers Templated by Melt Blowing Cocontinuous Immiscible Polymer Blends. *ACS Macro Lett.* **2021**, *10* (10), 1196–1203.
- (20) Pötschke, P.; Paul, D. R. Formation of Co-Continuous Structures in Melt-Mixed Immiscible Polymer Blends. *Journal of Macromolecular Science Polymer Reviews* **2003**, 43 (1), 87–141.
- (21) Pai, C. L.; Boyce, M. C.; Rutledge, G. C. Morphology of Porous and Wrinkled Fibers of Polystyrene Electrospun from Dimethylformamide. *Macromolecules* **2009**, 42 (6), 2102–2114.
- (22) Evans, N. T.; Irvin, C. W.; Safranski, D. L.; Gall, K. Impact of Surface Porosity and Topography on the Mechanical Behavior of High Strength Biomedical Polymers. *J. Mech Behav Biomed Mater.* **2016**, *59*, 459–473.
- (23) Zhang, Y.; Rodrigue, D.; Ait-Kadi, A. High Density Polyethylene Foams. III. Tensile Properties. J. Appl. Polym. Sci. 2003, 90 (8), 2130–2138.
- (24) Gibson, L. J.; Ashby, M. F. The Mechanics of Foams: Refinements. *Cellular Solids*; Cambridge University Press, 2014; pp 235–282. DOI: 10.1017/cbo9781139878326.008.
- (25) Pai, C. L.; Boyce, M. C.; Rutledge, G. C. Mechanical Properties of Individual Electrospun PA 6(3)T Fibers and Their Variation with Fiber Diameter. *Polymer* **2011**, *52* (10), 2295–2301.
- (26) Inai, R.; Kotaki, M.; Ramakrishna, S. Structure and Properties of Electrospun PLLA Single Nanofibres. *Nanotechnology* **2005**, *16* (2), 208–213.
- (27) Tan, E. P. S.; Ng, S. Y.; Lim, C. T. Tensile Testing of a Single Ultrafine Polymeric Fiber. *Biomaterials* **2005**, 26 (13), 1453–1456.

- (28) Wong, S. C.; Baji, A.; Leng, S. Effect of Fiber Diameter on Tensile Properties of Electrospun Poly(ε -Caprolactone). *Polymer* **2008**, 49 (21), 4713–4722.
- (29) Lim, C. T.; Tan, E. P. S.; Ng, S. Y. Effects of Crystalline Morphology on the Tensile Properties of Electrospun Polymer Nanofibers. *Appl. Phys. Lett.* **2008**, 92 (14), No. 141908.
- (30) Zervoudakis, A. J.; Sample, C. S.; Peng, X.; Lake, D.; Hillmyer, M. A.; Ellison, C. J. Dihydroxy Polyethylene Additives for Compatibilization and Mechanical Recycling of Polyethylene Terephthalate/Polyethylene Mixed Plastic Waste. *ACS Macro Lett.* **2022**, *11* (12), 1396–1402.
- (31) Quach, A.; Simha, R. Pressure-Volume-Temperature Properties and Transitions of Amorphous Polymers; Polystyrene and Poly (Orthomethylstyrene). J. Appl. Phys. 1971, 42 (12), 4592–4606.
- (32) Celanese. CELANEX 2008-PBT. https://tools.celanese.com/products/datasheet/SI/CELANEX%C2%AE%202008 (accessed 2023-01-05).
- (33) Bell, J. R.; Chang, K.; López-Barrón, C. R.; Macosko, C. W.; Morse, D. C. Annealing of Cocontinuous Polymer Blends: Effect of Block Copolymer Molecular Weight and Architecture. *Macromolecules* **2010**, 43 (11), 5024–5032.
- (34) Pan, Z.; Zhu, M.; Chen, Y.; Chen, L.; Wu, W.; Yu, C.; Xu, Z.; Cheng, L. The Variation of Fibrils' Number in the Sea-Island Fiber. *Fibers Polym.* **2010**, *11* (3), 494–499.
- (35) Macosko, C. W. Rheology Principles, Measurements and Applications; John Wiley & Sons, 1994.
- (36) Utracki, L. A. Melt Flow of Polymer Blends. *Polym. Eng. Sci.* **1983**, 23 (11), 602–609.
- (37) Chen, S.; Spruiell, J. E. Structure and Properties of High-speed Melt-spun Filaments of Poly(Butylene Terephthalate). *J. Appl. Polym. Sci.* **1987**, 33 (4), 1427–1444.
- (38) Yokouchi, M.; Sakakibara, Y.; Chatani, Y.; Tadokoro, H.; Tanaka, T.; Yoda, K. Structures of Two Crystalline Forms of Poly(Butylene Terephthalate) and Reversible Transition between Them by Mechanical Deformation. *Macromolecules* **1976**, 9 (2), 266–273.
- (39) De Rosa, C.; Auriemma, F.; Tarallo, O.; Malafronte, A.; Di Girolamo, R.; Esposito, S.; Piemontesi, F.; Liguori, D.; Morini, G. The "Nodular" α Form of Isotactic Polypropylene: Stiff and Strong Polypropylene with High Deformability. *Macromolecules* **2017**, *50* (14), 5434–5446.
- (40) Alberola, N.; Fugier, M.; Petit, D.; Fillon, B. Microstructure of Quenched and Annealed Films of Isotactic Polypropylene Part l. J. Mater. Sci. 1995, 30, 1187–1195.
- (41) Alberola, N.; Fugier, M.; Petit, D.; Fillon, B. Tensile Mechanical Behaviour of Quenched and Annealed Isotactic Polypropylene Films over a Wide Range of Strain Rates Part II Relationship with Microstructure. *J. Mater. Sci.* 1995, 30, 860–868.
- (42) Carr, P. L.; Jakeways, R.; Klein, J. L.; Ward, I. M. Tensile Drawing, Morphology, and Mechanical Properties of Poly (Butylene Terephthalate). *J. Polym. Sci. B Polym. Phys.* **1997**, 35 (15), 2465–2481.
- (43) Leclair, A.; Favis, B. D. The Role of Interfacial Contact in Immiscible Binary Polymer Blends and Its Influence on Mechanical Properties. *Polymer* **1996**, *37* (21), 4723–4728.
- (44) Gibson, L. J.; Ashby, M. F. The Mechanics of Foams: Basic Results. *Cellular Solids*; Cambridge University Press, 2014; pp 175–234. DOI: 10.1017/cbo9781139878326.007.
- (45) Tane, M.; Okamoto, R.; Nakajima, H. Tensile Deformation of Anisotropic Porous Copper with Directional Pores. *J. Mater. Res.* **2010**, 25 (10), 1975–1982.
- (46) Chen, M.; Zhu, J.; Qi, G.; He, C.; Wang, H. Anisotropic Hydrogels Fabricated with Directional Freezing and Radiation-Induced Polymerization and Crosslinking Method. *Mater. Lett.* **2012**. *89*, 104–107.
- (47) Herakovich, C. T.; Baxter, S. C. Influence of Pore Geometry on the Effective Response of Porous Media. *J. Mater. Sci.* **1999**, 34, 1595–1609.

- (48) Rice, R. W. Limitations of Pore-Stress Concentrations on the Mechanical Properties of Porous Materials. *J. Mater. Sci.* **1997**, 32, 4731–4736.
- (49) Ronan, W.; Deshpande, V. S.; Fleck, N. A. The Tensile Ductility of Cellular Solids: The Role of Imperfections. *Int. J. Solids Struct* **2016**, 102–103, 200–213.